

Joint Learning in the Gaussian Single Index Model

Loucas Pillaud-Vivien^{*} Adrien Schertzer[†]

June 9, 2025

Abstract

We consider the problem of jointly learning a one-dimensional projection and a univariate function in high-dimensional Gaussian models. Specifically, we study predictors of the form $f(x) = \varphi^*(\langle w^*, x \rangle)$, where both the direction $w^* \in \mathcal{S}_{d-1}$, the sphere of \mathbb{R}^d , and the function $\varphi^* : \mathbb{R} \rightarrow \mathbb{R}$ are learned from Gaussian data. This setting captures a fundamental non-convex problem at the intersection of representation learning and nonlinear regression. We analyze the gradient flow dynamics of a natural alternating scheme and prove convergence, with a rate controlled by the information exponent reflecting the *Gaussian regularity* of the function φ^* . Strikingly, our analysis shows that convergence still occurs even when the initial direction is negatively correlated with the target. On the practical side, we demonstrate that such joint learning can be effectively implemented using a Reproducing Kernel Hilbert Space (RKHS) adapted to the structure of the problem, enabling efficient and flexible estimation of the univariate function. Our results offer both theoretical insight and practical methodology for learning low-dimensional structure in high-dimensional settings.

1 Introduction

The problem of learning predictive functions from high-dimensional data lies at the heart of modern machine learning [2]. Among the vast landscape of models, *single-index* structures, wherein the target depends on the data only through a low-dimensional projection, have long captured both theoretical and practical attention [13, 4]. In their most canonical form, these models take the shape

$$x \mapsto \varphi^*(\langle w^*, x \rangle),$$

where $x \in \mathbb{R}^d$ denotes a high-dimensional input, $w^* \in \mathcal{S}_{d-1}$ is an unknown direction, and $\varphi^* : \mathbb{R} \rightarrow \mathbb{R}$ is an unknown univariate function [18, 26, 17]. This seemingly innocuous formulation conceals a rich interplay between geometry, approximation, and statistics [22, 5, 28].

The resurgence of interest in such models [15, 32, 30, 29] is fueled in part by their capacity to mirror the behavior of neural networks, especially in regimes where both the feature representations and the predictor are learned jointly. Indeed, when the function φ^* is parameterized flexibly—e.g., as an element of an infinite-dimensional space such as $L^2_\gamma(\mathbb{R})$ with respect to the Gaussian measure—the model transcends classical parametric confines and enters a semi-nonparametric realm that better captures the inductive biases of overparameterized networks [6].

In this work, we revisit single-index models through the lens of gradient flow. Our perspective is both analytic and algorithmic: we study the continuous-time dynamics induced by gradient descent when optimizing jointly over the direction w and the profile φ . To tame the infinite-dimensional nature of the problem, we exploit the Hermite basis, which offers a natural orthonormal expansion for functions in $L^2_\gamma(\mathbb{R})$. The resulting dynamics admit a concise spectral description, wherein the

^{*}CERMICS, Ecole Nationale des Ponts et Chaussées, Champs-sur-Marne, France. loucas.pillaud-vivien@enpc.fr

[†]Goethe University, Frankfurt am main, Germany. schertzer@hotmail.fr

evolution of each Hermite coefficient unfolds in a manner coupled to the geometric progression of the feature vector w .

Our contributions are threefold. First, we establish convergence guarantees for this joint gradient flow, characterizing its behavior via an *information exponent* [5, 11] that governs the amplification of informative components. In high dimension, the effect of random initialization becomes tractable: the initial alignment between w and the true direction w^* is of order $1/\sqrt{d}$, yet suffices to seed consistent recovery. Second, we dissect the dynamical coupling between direction learning and profile estimation, unveiling subtle mechanisms by which the two processes interact—sometimes harmoniously, sometimes antagonistically. Third, we introduce a practical implementation of this methodology using a reproducing kernel Hilbert space constructed from truncated Hermite expansions [14]. This allows us to interpolate between theoretical idealizations and algorithms amenable to numerical study.

Beyond the theoretical exposition, we corroborate our findings through a series of experiments, shedding light on the practical feasibility of this approach and validating our analytical predictions. Taken together, our results illuminate a path toward a principled understanding of joint learning in high dimensions, with ramifications for both the theory of neural networks and the design of new learning algorithms.

2 Problem Setup

We consider a high-dimensional learning problem in which the goal is to recover a predictive function from observations: i.e. random variables (X, Y) , where $X \in \mathbb{R}^d$ are high dimensional inputs and $Y \in \mathbb{R}$ is a scalar response. The data follow a single-index model [27] of the form

$$Y = \varphi^*(\langle w^*, X \rangle) + \varepsilon, \quad (1)$$

where: $X \sim \mathcal{N}(0, I_d)$ is a standard Gaussian vector in \mathbb{R}^d , $w^* \in \mathcal{S}_{d-1} \subset \mathbb{R}^d$ is an unknown unit-norm direction (the *index vector*), $\varphi^*: \mathbb{R} \rightarrow \mathbb{R}$ is an unknown measurable function (the *link function*), and ε is a zero-mean noise term, independent of X , with finite variance.

This setting defines a classical *single-index model* [26, 13], in which the response depends on the high-dimensional input only through the projection $\langle w^*, x \rangle$. Such models are of particular interest in high-dimensional statistics and machine learning, as they offer a structured form of dimensionality reduction while retaining modeling flexibility via the nonparametric function φ^* . For more details on these models, we refer to the recent review [9], and to [7, 12, 1] for multivariate extensions of these.

Function space. To reflect this flexibility, we assume that φ^* belongs to the Hilbert space $L_\gamma^2(\mathbb{R})$, where γ denotes the standard Gaussian measure on \mathbb{R} , and the inner product is given by

$$\langle f, g \rangle_{L_\gamma^2} := \int_{\mathbb{R}} f(z)g(z) d\gamma(z), \quad \text{where} \quad d\gamma(z) = \frac{1}{\sqrt{2\pi}} e^{-z^2/2} dz.$$

This choice is natural given that the latent variable $\langle w^*, X \rangle$ is itself standard Gaussian due to the isotropy of $X \in \mathbb{R}^d$ and the unit norm of w^* . It will also be useful to denote by \mathcal{H}_γ^j , the weighted Sobolev spaces $\mathcal{H}_\gamma^j := \{f \in L_\gamma^2, \text{ s.t. } f^{(j)} \in L_\gamma^2\}$, where $j \in \mathbb{N}$ and $f^{(j)}$ denote the j -th derivative of f . Obviously, this forms a nested structure of functional spaces: $L_\gamma^2 = \mathcal{H}_\gamma^0 \subset \mathcal{H}_\gamma^1 \subset \mathcal{H}_\gamma^2 \subset \dots$ of increasing regularity.

Model class. The learner has access to a class of predictors parameterized by a unit vector $w \in \mathcal{S}_{d-1}$ and a function $f \in L_\gamma^2(\mathbb{R})$. The model thus takes the form:

$$\mathcal{F} := \{f(\langle w, \cdot \rangle) \mid \text{for } w \in \mathcal{S}_{d-1} \text{ and } f \in L_\gamma^2(\mathbb{R})\},$$

which defines a semi-nonparametric family of predictors, combining a low-dimensional projection with an infinite-dimensional function class. The central object of study is the learning dynamics over this composite space.

Joint optimization. Our goal is to recover or approximate (w^*, φ^*) by minimizing the expected squared loss

$$\mathcal{L}(f, w) := \frac{1}{2} \mathbb{E} [(f(\langle w, X \rangle) - Y)^2], \quad (2)$$

over $f \in L^2_\gamma(\mathbb{R})$ and $w \in \mathcal{S}_{d-1}$. In this work, we focus on the gradient flow associated with \mathcal{L} , that is, the continuous-time limit of gradient descent updates over both w and f .

Hermite basis and structure of the loss. A crucial role in our analysis is played by the *Hermite polynomials* $(h_k)_{k \geq 0}$, which form a complete orthonormal basis of $L^2_\gamma(\mathbb{R})$, i.e. $\langle h_k, h_{k'} \rangle_{L^2_\gamma} = \delta_{kk'}$. For the sake of concreteness, we recall that for all $z \in \mathbb{R}$ $h_0(z) = 1$, $h_1(z) = z$, $h_2(z) = \frac{1}{2}(z^2 - 1) \cdots$, and that h_k is even (resp. odd) when k is (resp. odd) [8, Chapter 1.3]. Every square-integrable function $f \in L^2_\gamma(\mathbb{R})$ thus admits a unique expansion:

$$f(z) = \sum_{k=0}^{\infty} a_k h_k(z), \quad \text{with} \quad \sum_{k=0}^{\infty} a_k^2 = \|f\|_{L^2_\gamma}^2 < \infty.$$

This decomposition induces a natural coordinate system for analyzing gradient flows over f , as each Hermite component evolves in time in a coupled yet interpretable manner with the parameters w . Moreover, we can represent the spaces \mathcal{H}_γ^k with respect to summability assumption of the Hermite coefficients as $f \in \mathcal{H}_\gamma^j \Leftrightarrow \sum_{k \geq 0} k^{2j} |a_k|^2 < \infty$.

Lemma 1 (Loss expansion [13]). *The loss has the following expanded form*

$$\mathcal{L}(f, w) = \frac{1}{2} \|f\|_{L^2_\gamma}^2 + \frac{1}{2} \|\varphi^*\|_{L^2_\gamma}^2 - \sum_{k \geq 0} a_k a_k^* \langle w, w^* \rangle^k + \frac{1}{2} \text{Var}(\varepsilon), \quad (3)$$

That is to say that the loss rewrites $\mathcal{L}(f, w) = \ell(a, m)$, where

$$\ell(a, m) = \frac{1}{2} \sum_{k \geq 0} |a_k|^2 - \sum_{k \geq 0} a_k a_k^* \langle w, w^* \rangle^k + C_\varepsilon^*, \quad (4)$$

where $(a_k)_{k \in \mathbb{N}}, (a_k^*)_{k \in \mathbb{N}}$ are respectively the Hermite coefficients of f and φ^* , $m = \langle w, w^* \rangle \in [-1, 1]$ is the correlation and C_ε^* is a constant that does not depend on the model \mathcal{F} .

In the remaining of the article, for technical reasons, we shall assume that $\varphi^* \in \mathcal{H}^1$.

High-dimensional scaling. We are particularly interested in the high-dimensional regime where $d \gg 1$. In this setting, the inner product $\langle w, w^* \rangle$ between the true direction and a randomly initialized unit vector is typically of order $1/\sqrt{d}$, which induces a weak signal at initialization. Understanding how such weak alignment is amplified through the learning dynamics is central to our analysis.

Learning objective. The overarching question we seek to answer is the following:

Under what conditions, and at what rates, does the joint gradient flow over (w, f) recover the structure of the planted model (1)?

This entails both statistical and dynamical aspects: the identifiability of the target pair (w^*, φ^*) , and the behavior of the learning trajectory in the product space $\mathcal{S}_{d-1} \times L^2_\gamma$. In the sections that follow, we derive the gradient flow equations governing the evolution of (w_t, f_t) , analyze their convergence properties, and explore their practical realization via Hermite-based kernel methods.

3 Gradient Flow Dynamics

Gradient flow on $L_\gamma^2 \times \mathcal{S}_{d-1}$. In this section, we derive the equations of motions of the gradient flow on $\mathcal{L}(f, w)$. Hence, (at least formally for now), we say that $(f_t, w_t)_{t \geq 0}$ follow the gradient flow if they are solutions of the infinite dimensional system of ODEs

$$\frac{d}{dt} f_t = -\nabla_f^{L_\gamma^2} \mathcal{L}(f_t, w_t) , \quad (5)$$

$$\frac{d}{dt} w_t = -\nabla_w^{\mathcal{S}_{d-1}} \mathcal{L}(f_t, w_t) . \quad (6)$$

Let us explain the notation: for the parametric part, in order to leverage the rotation invariance of the Gaussian, we use the spherical gradient $\nabla_w^{\mathcal{S}_{d-1}} u(w) = \nabla_w u(w) - \langle w, \nabla_w u(w) \rangle w$ for any differentiable function u . For the non-parametric part, we use the Hilbert property of $(L_\gamma^2, \langle \cdot, \cdot \rangle_{L_\gamma^2})$ and Riesz theorem to represent the Fréchet differential of $\mathcal{L}(\cdot)$ in terms of a gradient, i.e. for all g sufficiently smooth,

$$\left\langle \nabla_f^{L_\gamma^2} \mathcal{L}(f, w), g \right\rangle_{L_\gamma^2} = \lim_{h \rightarrow 0} \frac{\mathcal{L}(f + hg, w) - \mathcal{L}(f, w)}{h} . \quad (7)$$

Dynamics on $\ell_2(\mathbb{N}) \times [-1, 1]$. Now that the gradient flow is (at least at the formal level) well-defined, we show that this flow on $(f_t, w_t)_{t \geq 0} \in L_\gamma^2 \times \mathcal{S}_{d-1}$ induces equations of movement on the reduced parameters $((a_{k,t})_{k \in \mathbb{N}}, m_t)_{t \geq 0} \in \ell_2(\mathbb{N}) \times [-1, 1]$. In fact, the gradient structure on f in the space L_γ^2 reduces to the Hilbert gradient structure on $\ell_2(\mathbb{N})$ for the coefficient $(a_k)_{k \in \mathbb{N}}$ of f . This corresponds to the infinite system of ODEs stated in the following Lemma.

Lemma 2. *Let $(f_t, w_t)_{t \geq 0}$ follow the gradient flow Eqs.(5)-(6), then*

$$\frac{d}{dt} a_{k,t} = a_k^* m_t^k - a_{k,t} , \text{ for all } k \in \mathbb{N} , \quad (8)$$

$$\frac{d}{dt} m_t = (1 - m_t^2) \sum_{k=1}^{\infty} k a_{k,t} a_k^* m_t^{k-1} , \quad (9)$$

where $m_t = \langle w_t, w^* \rangle$ and $f_t := \sum_{k \geq 0} a_{k,t} h_k$.

Initialization and information exponent. We use a non-informed initialization to the problem. For the parametric part, we initialize according to the uniform distribution on the sphere. A striking consequence of this is that the correlation between initialization w_0 and the true direction w^* is of order $1/\sqrt{d}$. Indeed, it is a standard result that with overwhelming probability, we have $c/\sqrt{d} \leq |\langle w_0, w^* \rangle| \leq C/\sqrt{d}$, with $c, C > 0$ two positive constants. Hence, when running the algorithm in practice, it is initialized with a high probability near the equator of \mathcal{S}_{d-1} , or at least in a band of typical size $1/\sqrt{d}$. Let

$$s = \inf \{ k \in \mathbb{N}^* \mid a_k^* \neq 0 \} \quad (10)$$

be the *information exponent* [5] of φ^* . The value of this integer crucially controls the behavior of the dynamics, as we will see in the main result. Indeed, we see from Eq.(9), that at initialization the movement of m is governed by the ODE $\dot{m}_t \sim a_{s,t} m_t^{s-1}$, whose typical time to escape a neighborhood of the origin depends highly on how large the exponent s is. For the non-parametric part, we use an initialization on the coefficient in the Hermite basis directly and initialize such that $k^2 a_{k,0} \sim \mathcal{U}([-1, 1])$. Note that thus we have $f_0 = \sum_{k \geq 0} a_{k,0} h_k \in \mathcal{H}^2$ almost surely.

Comparison with the planted model. In the idealized *planted model* setting, where φ^* is known in advance (e.g., $f_t = \varphi^*$ or equivalently $a_{k,t} = a_k^*$ held fixed), Equation (9) becomes a closed-form ODE for m_t . In this case, it can be shown that: (i) if $m(0) > 0$, the alignment is reinforced and $m_t \rightarrow 1$, (ii) if $m(0) < 0$, in some cases, the gradient flow converges to the origin or to the first negative zero of the power series $x \rightarrow \sum_{k=1}^{\infty} k(a_k^*)^2 x^{k-1}$ and in either case w fails to recover w^* . We highlight this result in Proposition 1.

This stark asymmetry illustrates a surprising and important fact: *in the planted model, negative initial correlation cannot be corrected by the dynamics*. The flow becomes trapped at a fixed point, even though the loss function has a global minimum at $m = 1$. In the joint learning setting, where f is learned simultaneously, the dynamics are more subtle and can escape such traps—this is a key motivation for the joint approach.

Summary. In summary, the gradient flow system evolves over the product space $\mathcal{S}_{d-1} \times \ell^2(\mathbb{N})$, with dynamics governed by the coupled ODEs given in Lemma 2. These equations encode a feedback loop: the alignment m_t controls the effective signal in the functional update, while the function f_t , in turn, modulates the reinforcement of alignment through the coefficients $a_{k,t}$. The initialization of the correlation, of order $1/\sqrt{d}$, structures the dynamics near the origin, where the time scales are expected to be controlled by the information exponent s .

The precise resolution of this interaction is the subject of the next section, where we analyze the convergence behavior.

4 Convergence Behavior of the Joint Gradient Flow

Understanding the asymptotic behavior of the gradient flow dynamics, especially in the high-dimensional setting, is central to this work. We begin by recalling known results on the so-called *planted model*, in which the target function $\varphi^* \in L^2_\gamma$ is fixed and known in advance, and the gradient flow acts only on the feature direction $w \in \mathcal{S}_{d-1}$. This model serves as an instructive warm-up, showing that when the initialization $m_0 := \langle w_0, w^* \rangle$ is negatively correlated, the system fails to recover the signal. It also prepares the ground for the more involved dynamics of joint learning over both w and f .

The Planted Model. In this case, the dynamics reduce to a one-dimensional ordinary differential equation for the correlation $m_t := \langle w_t, w^* \rangle$, as previously derived:

$$\dot{m}_t = (1 - m_t^2) \sum_{k=1}^{\infty} k(a_k^*)^2 m_t^{k-1},$$

where a_k^* are the Hermite coefficients of the function φ^* . Let $\Phi(x) := \sum_{k=1}^{\infty} k(a_k^*)^2 x^{k-1}$, and \mathcal{Z}_Φ the set of zeros of Φ on $[-1, 1]$. Then, it is clear that $\mathcal{Z}_\Phi \cap \mathbb{R}_{>0} = \emptyset$. When $\mathcal{Z}_\Phi \cap \mathbb{R}_{<0} \neq \emptyset$, we define $\bar{m} = \min\{|z| \mid z \in \mathcal{Z}_\Phi \cap \mathbb{R}_{<0}\}$, and if $\mathcal{Z}_\Phi \cap \mathbb{R}_{<0} = \emptyset$, we set $\bar{m} = +\infty$ and then we have the following proposition.

Proposition 1 (Bifurcations in the planted model). *Let m_t evolve under the planted gradient flow with fixed target function $\varphi^* \in L^2_\gamma$, and let $m_0 := \langle w_0, w^* \rangle$ denote the initial correlation. Then:*

- If $m_0 > 0$, the trajectory converges to alignment: $\lim_{t \rightarrow \infty} m_t = 1$.
- If $m_0 < 0$, then, (i) if $s \geq 3$ is odd, we have $\lim_{t \rightarrow \infty} m_t = 0$;
 else, (ii) if s is even, then
 - If $\bar{m} > 1$, the trajectory converges to anti-alignment: $\lim_{t \rightarrow \infty} m_t = -1$.

– If $\bar{m} < 1$, the trajectory remains trapped in a local minimizer and $\lim_{t \rightarrow \infty} m_t = -\bar{m}$.

This behavior is folklore in the literature [5, 7, 10, 31] and the result could be enhanced by proving convergence rate, but we decide not to state them here, as the only purpose of this proposition is to show that the system could lead to learning failure in the case $m_0 < 0$. This bifurcation highlights a fundamental limitation of the planted gradient flow: although the global minimum of the loss is achieved at $m = 1$, in some cases, the dynamics cannot escape the spurious basin of attraction when the initial correlation is negative. In contrast, as we shall now demonstrate, the joint learning dynamics over both w and f exhibit a markedly different behavior, one which allows the system to overcome this initialization asymmetry.

4.1 Main theorem: convergence in the Joint Learning Setting

We now turn to the full gradient flow over the product space $\mathcal{S}_{d-1} \times L_\gamma^2$, where both the direction w_t and the profile function f_t evolve jointly. As we have seen, the dynamics can be decomposed spectrally in the Hermite basis, with coefficients $a_{k,t} := \langle f_t, h_k \rangle$, and the correlation $m_t := \langle w_t, w^\star \rangle$. The coupled evolution equations are given in Eqs.(8)-(9).

These dynamics reveal a feedback mechanism: the function f_t becomes gradually aligned with the true target φ^\star , but only to the extent that the correlation m_t allows it to see the correct Hermite modes. In turn, the recovery of the direction w_t depends on the functional alignment via the second equation.

Remarkably, this feedback loop can break the symmetry obstruction observed in the planted case. The next two theorems provide a rigorous characterization of the convergence behavior in the joint learning setting, depending on the regularity exponent s of the target function φ^\star .

Theorem 1. *Let (m, a) follows equations Eqs.(8)-(9). Then, with overwhelming probability on the initialization, taken as described in the previous section, there exists constants $c, C > 0$ so that,*

Case $s \geq 2$. After time $t \geq \tau_c \geq Cd^{s-1}$,

$$\bullet \text{ if } m_0 > 0, \quad |1 - m_t| \leq Ce^{-c(t-\tau_c)}, \quad (11)$$

$$|a_{k,t} - a_k^\star| \leq Cb_k e^{-c(t-\tau_c)}, \text{ for all } k \in \mathbb{N}, \quad (12)$$

$$\bullet \text{ if } m_0 < 0, \quad |1 + m_t| \leq Ce^{-c(t-\tau_c)}, \quad (13)$$

$$|a_{k,t} - (-1)^k a_k^\star| \leq Cb_k e^{-c(t-\tau_c)}, \text{ for all } k \in \mathbb{N}, \quad (14)$$

Case $s = 1$. After time $t \geq 0$,

$$\bullet \text{ if } a_1^\star a_{1,0} > 0, \quad |1 - m_t| \leq Ce^{-ct}, \quad (15)$$

$$|a_{k,t} - a_k^\star| \leq Cb_k e^{-ct}, \text{ for all } k \in \mathbb{N}, \quad (16)$$

$$\bullet \text{ if } a_1^\star a_{1,0} < 0, \quad |1 + m_t| \leq Ce^{-ct}, \quad (17)$$

$$|a_{k,t} - (-1)^k a_k^\star| \leq Cb_k e^{-ct}, \text{ for all } k \in \mathbb{N}, \quad (18)$$

where, $b \geq 0$ is a normalized sequence of $\ell_2(\mathbb{N})$, i.e. $\|b\|_{\ell_2(\mathbb{N})} = 1$.

Theorem 1 offers a precise characterization of the long-time behavior of the joint gradient flow in the Hermite basis. The evolving state of the system is described by the pair (m_t, a_t) , where $m_t := \langle w_t, w^\star \rangle \in [-1, 1]$ tracks the alignment between the current direction $w_t \in \mathbb{S}^{d-1}$ and the planted direction w^\star , while $a_{k,t} := \langle f_t, h_k \rangle$ are the Hermite coefficients of the profile function $f_t \in L_\gamma^2$.

We distinguish two regimes depending on the index $s \in \mathbb{N}^*$, which is defined as the smallest integer $s \geq 1$ such that $a_s^\star \neq 0$. In other words, s corresponds to the leading nonzero mode in the Hermite expansion of the target function φ^\star . This parameter controls the initial signal strength in the direction dynamics, and determines both the presence and the duration of the transient phase before

convergence. Finally, the coefficients that converge toward a zero target value exhibit exponentially fast convergence to zero, uniformly in time and independently of the dimension.

Case $s \geq 2$. Delayed convergence due to weak initialization. In this case, the first nonzero coefficient a_s^* appears at index $s \geq 2$. As a result, the initial gradient signal in the direction w is weak, scaling like m_0^{s-1} . The theorem asserts the existence of a *concentration time* $\tau_c \geq m_0^{-2(s-1)} \sim d^{s-1}$, beyond which the system enters an exponential convergence phase. In fact, τ_c is the time needed for *weak recovery*, i.e. the time at which m reaches a level set independent of the dimension. We actually prove in Lemma 6 in the Appendix that there exist $b, B > 0$, such that $bd^{(s-1)} \leq \tau_c \leq Bd^{(s-1)}$, from which we deduce that

$$\tau_c \sim d^{s-1}. \quad (19)$$

After time $t \geq \tau_c$, the flow converges toward one of two symmetric attractors: (i) if $m_0 > 0$, then $m_t \rightarrow 1$, and $a_{k,t} \rightarrow a_k^*$, or (ii) if $m_0 < 0$, then $m_t \rightarrow -1$, and $a_{k,t} \rightarrow (-1)^k a_k^*$, with rates governed by an exponentially decaying envelope modulated by a sequence $b \in \ell_2(\mathbb{N})$, normalized as $\|b\|_{\ell_2} = 1$. The key phenomenon is that the joint dynamics enable recovery regardless of the sign of m_0 , provided one waits long enough. In contrast to the planted model, where negative initialization traps the flow in a spurious basin, here the adaptive evolution of the function f_t corrects for early misalignment.

Case $s = 1$. Immediate convergence. In the special case $s = 1$, the first Hermite coefficient a_1^* is already active. This injects a strong signal into the direction dynamics from the outset, and no transient phase is needed. The convergence is exponential for all $t \geq 0$, with rate independent of dimension. The basin of attraction is now determined by the sign of the product $a_{1,0}a_1^*$, i.e., whether the initial function f_0 shares the correct sign on the leading mode. If this product is positive, the system converges to $m_t \rightarrow 1$, and if negative, to $m_t \rightarrow -1$, with corresponding flips in the sign pattern of the Hermite coefficients.

The essential quantity that governs recovery is not the individual convergence of m_t or $a_{k,t}$, but rather the convergence of their product: $a_{k,t} m_t^k \rightarrow a_k^*$, as $t \rightarrow \infty$. This is the quantity that enters into the effective representation $f_t(\langle w_t, x \rangle)$, and determines the predictive performance of the model. Since $m_t^k \rightarrow (\pm 1)^k$ and $a_{k,t} \rightarrow (\pm 1)^k a_k^*$, we obtain in both cases:

$$f_t(\langle w_t, x \rangle) = \sum_{k=0}^{\infty} a_{k,t} h_k(\langle w_t, x \rangle) \rightarrow \sum_{k=0}^{\infty} a_k^* h_k(\langle w^*, x \rangle) = \varphi^*(\langle w^*, x \rangle),$$

regardless of the sign of m_0 . Thus, the flow achieves perfect recovery of the target regression function in the limit $t \rightarrow \infty$, even though the feature direction w_t may converge to either $+w^*$ or $-w^*$, depending on the initialization.

4.2 Description of the dynamics and sketch of the proof

We now describe and break down the dynamics of the system distinguishing between the case $s \geq 2$ and the case $s = 1$, which behaves differently. Initially, recall that m_t is very close to zero on a scale of order $1/\sqrt{d}$.

Case $s \geq 2$. The dynamics happens in different phases:

- (i) **Phase I: rapid movement of $a_{k,t}$ towards $a_k^* m_t^k$.** On the one hand, in the dynamics of m , initially, the vector field is of intensity m^{s-1} at first order. Hence, m_t remains very close to the

initialization for a time, at least of order m_0^{1-s} . On the other hand, given Eq. (8), the movement of a_k corresponds to an exponentially fast shrinkage at rate 1 until it hits the neighborhood of $a_k^* m_t^k$. Hence, during this period, an arbitrary number k^* of coefficients $a_{k,t}$ partially stabilize toward $a_k^* m_t^k$ within a time t_{k^*} of order $k^* \log(1/m_0)$. The slow dynamics of m_t , compared to the fast dynamics of $a_{k,t}$ (fast-slow dynamics), allows the system to achieve a *positivity principle*. Indeed, in light of equation Eq.(9), it is now clear to see that m_t increases if m_0 is positive (respectively decreasing if m_0 is negative) from t_{k^*} . In fact, the terms corresponding to the indices larger than k^* do not contribute to the dynamics, as they correspond to the remainder of a converging series.

- (ii) **Phase II: slow increase of m .** The dynamics stabilizes in virtue of the *positivity principle* and for a constant c independent of the dimension, we have $\dot{m}_t \sim cm^{2s-1}$ until the system reaches this constant. We deduce that reaching this constant takes a time of order $m_0^{-2(s-1)} \sim d^{s-1}$.
- (iii) **Phase III: exponential convergence.** After that, the dynamics of the order parameter m_t becomes independent of the initial value and converges exponentially fast as the $a_{k,t}$ follow the lead.

Case $s = 1$. This case works quite differently from the previous one. In virtue of Eq.(8), $a_{1,t}$ partially stabilizes towards $a_1^* m_t$. However, this time, m_t follows the fast dynamics. Indeed, initially, m_t will move linearly toward $a_0^* a_{1,0}$: Thus, m_t adapts to the sign of $a_1^* a_{1,0}$ without any time dependence on m_0 , while $a_{1,t}$ will not be able to change its sign. After this, m_t will no longer change its sign. After a time independent of the initial condition, the system reaches again a *positivity principle* as in the previous case.

5 Kernel Implementation via Hermite Functions

The procedure described above considers an idealized scenario, where the non-parametric regression is performed on the whole ambient space L_γ^2 . We show that this can be practically carried by performing this non-parametric regression on a dense Reproducing Kernel Hilbert Space $\mathcal{H} \subset L_\gamma^2$, written as RKHS in short, see [23, 25] for an overview.

A Hermite dense RKHS. First, we construct such a RKHS space, adapted to the Hermite structure of our problem. To do this let us define $(c_k)_{k \in \mathbb{N}} \in \ell_2(\mathbb{N})$ a positive sequence. Furthermore, we ask that $\sum_k k c_k < +\infty$, that is to say that c has some fast decay at infinity, e.g. $c_k = o(k^{-2})$. Then, we use the following construction.

Proposition 2. *For all sequences $(c_k)_{k \in \mathbb{N}}$ defined as previously, the subspace*

$$\mathcal{H} := \left\{ f \in L_\gamma^2 \cap \mathcal{C}(\mathbb{R}^q) ; \text{ such that } \|f\|_{\mathcal{H}}^2 := \sum c_k^{-1} a_k^2 < +\infty \right\} \quad (20)$$

defines a dense RKHS with kernel $K(x, y) = \sum_k c_k h_k(x) h_k(y) = \langle \phi(x), \phi(y) \rangle_{\ell_2}$, where the equality stands in a point-wise sense and $\phi_k = \sqrt{c_k} h_k$. Finally, we also define, for any $f, g \in \mathcal{H}$, the inner product $\langle f, g \rangle_{\mathcal{H}} := \sum_\beta c_\beta^{-1} \langle f, h_\beta \rangle \langle g, h_\beta \rangle$.

Note that similar RKHSs have already been considered for numerical computation of expectation with respect to Brownian paths, e.g. [16] and statistical estimation of multi-index problems [14]. We refer to the first cited paper for the construction as well as more on smoothness properties of such RKHSs. The RKHS norm $\|f\|_{\mathcal{H}}^2$ is thus of the form $\sum_k c_k^{-1} \langle f, h_k \rangle^2$, and therefore defines a weighted Sobolev space, similar to \mathcal{H}^p , if c decreases as a power law. Note also that it is possible to use a random process to express the kernel, as it has been already pinned as a *random feature expansion of the kernel* [21] (see [7] for such a construction). Note that this could also lead to some regularization,

by considering the loss $\mathcal{L}(f, w) + \mu \|f\|_{\mathcal{H}}^2/2$ that would act as a threshold of the high frequencies of the function φ^* .

Approximation with finite dimensional RKHS. Obviously, one can define for any integer $k \in \mathbb{N}^*$, a finite dimensional RKHS that we will denote \mathcal{H}_k by truncating the feature map ϕ as $\phi_k = (\sqrt{c_0}h_0, \sqrt{c_1}h_1, \dots, \sqrt{c_k}h_k) \in \mathbb{R}^{k+1}$. This enables in practice to run the gradient flow on $((a_k)_{k \leq k}, m)$ as a true ODE, or a numerical method, by discretizing it via a Euler scheme that fits on a computer. Obviously, the larger the k , the better the approximation will be as for any $f \in \mathcal{H}^1$,

$$\inf_{g \in \mathcal{H}_k} \|f - g\|_{L^2_\gamma}^2 = \sum_{k \geq k+1} a_k^2 \leq \sqrt{\sum_{k \geq k+1} k^2 a_k^2} \sqrt{\sum_{k \geq k+1} \frac{a_k^2}{k^2}} \leq \frac{\|f\|_{\mathcal{H}^1}^2}{k^2}.$$

This is what is done practically as pictured in the following section.

6 Numerical Experiments

To validate and illustrate our theoretical findings, we present two sets of numerical experiments. The first set directly discretizes the idealized gradient flow equations derived in the infinite-dimensional, population-risk setting, whereas the second set considers the empirical loss and finite-dimensional approximation described in Section 5. Both experiments aim to shed light on the characteristic fast–slow dynamics of the system and the role of the symmetry-breaking in the joint learning process.

Simulation of the idealized dynamics. In this first set of experiments, we study the discretized gradient flow equations for the scalar coefficients $a_{k,t}$ and the alignment parameter $m_t := \langle w_t, w^* \rangle$, in the regime where the planted function corresponds to $\varphi^* = h_2 + h_3 - h_4$, i.e., a linear combination of Hermite polynomials up to degree four. This choice corresponds to the setting $s = 2$, meaning that the first nonzero Hermite coefficient is $a_2^* = 1$. We initialize the correlation at a very small positive value $m_0 \sim 10^{-4}$ to mimic the weak alignment typically induced by high-dimensional random initialization (e.g., when $w_0 \sim \text{Unif}(\mathcal{S}_{d-1})$ with $d \gg 1$). The coefficients $a_{k,0}$ are initialized to $\{\pm 1\}$ for all $k \leq k$. Figure 1 displays the phase portrait of the dynamics of $(m_t, a_{4,t})$ planes, along with the full learning curve of m_t and $a_{4,t}$ over time¹. We observe a sharp transition in behavior, in line with the theory developed for the case $s \geq 2$. Note that as long as $m, a_4 \ll 1$, the phase portrait perfectly follows the curve $x = -y^4$ (in green in Figure 1), showing that at this stage that last a time of order d^{s-1} , the dynamics reaches a partial equilibrium in terms of a .

¹We picked at random the coefficient $a_{k,t}$ to be shown, the behavior of the other are similar.

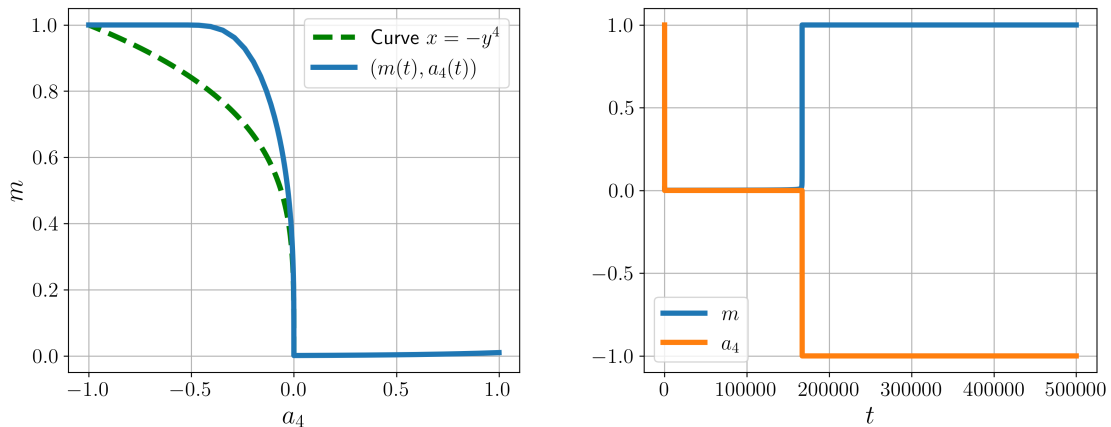
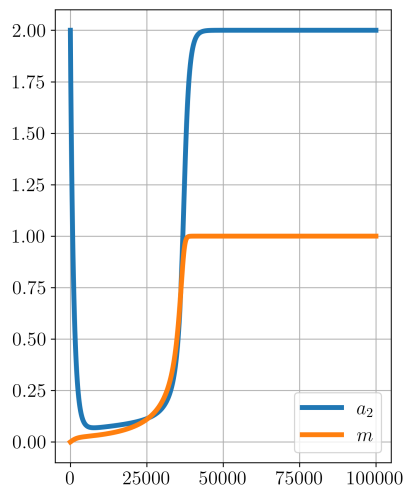


Figure 1: At early stages, the weak signal from m_0 induces a fast decay of the coefficient $a_{4,t}$, which acts as a passive mode. Then, the dynamics enters a phase of partial equilibrium (slow-fast dynamics), where $a_{k,t} \simeq a_k^* m_t^k$ and m_t grows very slowly. Once m_t crosses a critical threshold, the dynamics switch regimes and $a_{4,t}$ begins to grow, reinforcing the directional alignment.

Empirical RKHS-based dynamics. In the second set of experiments, we implement the joint learning procedure in the practical setting described in Section 5. The function class is represented by a finite-dimensional truncation of the Hermite-based RKHS, and the empirical risk is minimized via standard gradient descent. We generate a dataset of $n = 10^5$ i.i.d. Gaussian inputs in dimension $d = 10^2$, with labels computed from the planted function $\varphi^*(x) = 2h_2(\langle w^*, x \rangle)$, and run gradient descent on the empirical loss using the RKHS parameterization. Both the direction w_t and the coefficients $a_{k,t}$ are updated jointly. Figure 6 shows the evolution of the alignment m_t , as well as the coefficient $a_{2,t}$, as a function of time. The qualitative behavior closely matches the idealized dynamics described earlier, which seems to imply that with enough samples, and small enough step size, the empirical dynamics and the idealized one match.



These experiments confirm that the key phenomena predicted in the population-risk regime persist in the finite-sample setting, even under stochastic initialization and discretization. They also validate the practical relevance of the RKHS-based modeling approach for analyzing learning in single-index neural architectures.

7 Conclusion and Outlook

In this work, we have analyzed the dynamics of a joint gradient flow designed to learn a univariate function of a linear projection. The evolution of the system exhibits a striking separation of timescales between the nonparametric learning of the scalar function and the estimation of the projection direction. This separation gives rise to a fast-slow dynamical regime, especially pronounced in high

dimensions and for complex target functions. A particularly intriguing outcome of our analysis is that joint learning—despite its apparent lack of structural knowledge—can outperform scenarios in which the target function is fixed *a priori*. In some cases, fixing the function can trap the dynamics in a suboptimal basin, whereas the flexibility of joint learning allows the system to escape such traps and achieve global convergence. This behavior echoes a broader phenomenon observed in overparameterized models, such as neural networks, where learning flexibility often aids in finding better minima.

With the temporal structure of the flow now well understood, a natural next step is to investigate the *sample complexity* of joint learning [11, 19]. Our analysis has so far focused on the infinite-sample (population) regime, but practical implementations rely on finite datasets [20], with a finite truncation of the Hermite expansion and a discrete-time algorithm. In such settings, both the estimation of the functional coefficients $a_{k,t}$ and the evolution of the correlation parameter m_t are impacted by statistical noise and generalization error. Quantifying the number of samples required to reliably recover the target coefficients and ensure convergence is thus an essential direction for future work. In particular, it is important to understand how this sample complexity depends on the initialization m_0 , the number of learned coefficients, and the spectral structure of the target [5]. Such an analysis would bridge the gap between the idealized continuous-time dynamics studied here and the finite-data, discrete-time algorithms employed in practice. Ultimately, this could lead to a rigorous understanding of stochastic gradient descent in the joint learning setting, whose covariance noise structure [24] should play a prominent role during the early times.

Acknowledgments. A. S. acknowledges support by the Deutsche Forschungsgemeinschaft (DFG, German Research Foundation)- project number 432176920. L.P-V. acknowledges support by the Fondation Beout.

References

- [1] Emmanuel Abbe, Enric Boix-Adsera, and Theodor Misiakiewicz. Sgd learning on neural networks: leap complexity and saddle-to-saddle dynamics. *Proceedings of Machine Learning Research*, 195:1–72, 2023.
- [2] Francis Bach. *Learning theory from first principles*. MIT press, 2024.
- [3] Dominique Bakry, Ivan Gentil, and Michel Ledoux. *Analysis and geometry of Markov diffusion operators*, volume 348. Springer Science & Business Media, 2013.
- [4] Gerard Ben Arous, Reza Gheissari, and Aukosh Jagannath. Online stochastic gradient descent on non-convex losses from high-dimensional inference. *J. Mach. Learn. Res.*, 22:106–1, 2021.
- [5] Gerard Ben Arous, Reza Gheissari, and Aukosh Jagannath. High-dimensional limit theorems for sgd: Effective dynamics and critical scaling. *Advances in neural information processing systems*, 35:25349–25362, 2022.
- [6] Raphaël Berthier, Andrea Montanari, and Kangjie Zhou. Learning time-scales in two-layers neural networks. *Found Comput Math*, 2024.
- [7] Alberto Bietti, Joan Bruna, and Loucas Pillaud-Vivien. On learning gaussian multi-index models with gradient flow. *arXiv preprint arXiv:2310.19793*, 2023.
- [8] Vladimir Igorevich Bogachev. Gaussian measures. *American Mathematical Soc.*, 36(62), 1998.
- [9] Joan Bruna and Daniel Hsu. Survey on algorithms for multi-index models. *arXiv preprint arXiv:2504.05426*, 2025.

- [10] Alex Damian, Eshaan Nichani, Rong Ge, and Jason D Lee. Smoothing the landscape boosts the signal for sgd: Optimal sample complexity for learning single index models. *Proceedings of the 37th International Conference on Neural Information Processing Systems*, 2023.
- [11] Alex Damian, Loucas Pillaud-Vivien, Jason D Lee, and Joan Bruna. Computational-statistical gaps in gaussian single-index models. *arXiv preprint arXiv:2403.05529*, 2024.
- [12] Yatin Dandi, Florent Krzakala, Bruno Loureiro, Luca Pesce, and Ludovic Stephan. Learning two-layer neural networks, one (giant) step at a time. *Journal of Machine Learning Research*, 2024.
- [13] Rishabh Dudeja and Daniel Hsu. Learning single-index models in gaussian space. In Sébastien Bubeck, Vianney Perchet, and Philippe Rigollet, editors, *Proceedings of the 31st Conference On Learning Theory*, volume 75 of *Proceedings of Machine Learning Research*, pages 1887–1930. PMLR, 06–09 Jul 2018.
- [14] Bertille Follain, Umut Simsekli, and Francis Bach. Nonparametric linear feature learning in regression through regularisation. *arXiv preprint arXiv:2307.12754*, 2023.
- [15] Spencer Frei, Yuan Cao, and Quanquan Gu. Agnostic learning of a single neuron with gradient descent. *Advances in Neural Information Processing Systems*, 33:5417–5428, 2020.
- [16] Christian Irrgeher and Gunther Leobacher. High-dimensional integration on rd, weighted hermite spaces, and orthogonal transforms. *Journal of Complexity*, 31(2):174–205, 2015.
- [17] Sham M Kakade, Varun Kanade, Ohad Shamir, and Adam Kalai. Efficient learning of generalized linear and single index models with isotonic regression. *Advances in Neural Information Processing Systems*, 24, 2011.
- [18] Adam Tauman Kalai and Ravi Sastry. The isotron algorithm: High-dimensional isotonic regression. In *COLT*, 2009.
- [19] Antoine Maillard, Bruno Loureiro, Florent Krzakala, and Lenka Zdeborová. Phase retrieval in high dimensions: Statistical and computational phase transitions. *Advances in Neural Information Processing Systems*, 33:11071–11082, 2020.
- [20] Song Mei, Yu Bai, and Andrea Montanari. The landscape of empirical risk for nonconvex losses. *The Annals of Statistics*, 46(6A):2747–2774, 2018.
- [21] Ali Rahimi and Benjamin Recht. Random features for large-scale kernel machines. *Advances in neural information processing systems*, 20, 2007.
- [22] David Saad and Sara A Solla. Exact solution for on-line learning in multilayer neural networks. *Physical Review Letters*, 74(21):4337, 1995.
- [23] Robert Schaback and Holger Wendland. Kernel techniques: from machine learning to meshless methods. *Acta numerica*, 15:543–639, 2006.
- [24] Adrien Schertzer and Loucas Pillaud-Vivien. Stochastic differential equations models for least-squares stochastic gradient descent. *arXiv:2407.02322*, 2024.
- [25] Bernhard Schölkopf and Alexander Smola. *Learning with kernels: support vector machines, regularization, optimization, and beyond*. MIT press, 2002.
- [26] Shai Shalev-Shwartz, Ohad Shamir, and Karthik Sridharan. Learning kernel-based halfspaces with the zero-one loss. *SIAM J. COMPUT.*, 2010.

- [27] Mahdi Soltanolkotabi. Learning relus via gradient descent. *Advances in neural information processing systems*, 2017.
- [28] Rodrigo Veiga, Ludovic Stephan, Bruno Loureiro, Florent Krzakala, and Lenka Zdeborová. Phase diagram of stochastic gradient descent in high-dimensional two-layer neural networks. *arXiv preprint arXiv:2202.00293*, 2022.
- [29] Lei Wu. Learning a single neuron for non-monotonic activation functions. In *International Conference on Artificial Intelligence and Statistics*, pages 4178–4197. PMLR, 2022.
- [30] Gilad Yehudai and Ohad Shamir. Learning a single neuron with gradient methods. In *Conference on Learning Theory*, pages 3756–3786. PMLR, 2020.
- [31] Aaron Zweig and Joan Bruna. Symmetric single index learning. *arXiv preprint arXiv:2310.02117*, 2023.
- [32] Aaron Zweig, Loucas Pillaud-Vivien, and Joan Bruna. On single-index models beyond gaussian data. *Advances in Neural Information Processing Systems*, 36:10210–10222, 2023.

Appendix

The appendix is organized as follows:

- We first present the proof of Lemma 1 in Section A, which concerns the form of the loss.
- In Section B, we prove Lemma 2, which describes the dynamics of the Hermite coefficients and the order parameter m .
- At the beginning of Section C, we look at the limitation of the dynamics for the planted model and prove Proposition 1.
- The rest of Section C is dedicated to the proof of the joint dynamics, which corresponds to Theorem 1.

In the following, the constants c and C denote dimension-independent constants whose values may change from line to line throughout the proofs.

A Problem Setup

We begin by proving Lemma 1 about the expansion of the loss.

Proof of Lemma 1. We first recall that

$$\begin{aligned} \mathcal{L}(f, w) &= \frac{1}{2} \mathbb{E} [(f(\langle w, X \rangle) - \varphi^*(\langle w^*, X \rangle) - \varepsilon)^2] \\ &= \frac{1}{2} \|f\|_{L^2_\gamma}^2 + \frac{1}{2} \|\varphi^*\|_{L^2_\gamma}^2 + \frac{1}{2} \text{Var}(\varepsilon) - \mathbb{E} [(f(\langle w, X \rangle) \varphi^*(\langle w^*, X \rangle))] , \end{aligned}$$

by developing the square and using the fact that $\langle w, X \rangle \sim \langle w^*, X \rangle \sim \mathcal{N}(0, 1)$ and that ε is independent of X . We recall that our analysis is based on the *Hermite polynomials* $(h_k)_{k \geq 0}$, which form a complete orthonormal basis and we deduce that

$$\|f\|_{L^2_\gamma}^2 = \sum_{k=0}^{+\infty} a_k^2 .$$

In addition, one readily check that

$$\text{Cov}(\langle w, X \rangle, \langle w^*, X \rangle) = \langle w, w^* \rangle =: m ,$$

and by a simple covariance calculation, we obtain

$$\begin{aligned} \mathbb{E} [f(\langle w, X \rangle) \varphi^*(\langle w^*, X \rangle)] &= \mathbb{E}_{Y, Z} \left[f(Y) \varphi^*(mY + \sqrt{1 - m^2}Z) \right] \\ &= \mathbb{E}_Y \left[f(Y) \mathbb{E}_Z \varphi^*(mY + \sqrt{1 - m^2}Z) \right] , \end{aligned}$$

where Y, Z are i.i.d. standard Gaussian. A fundamental fact is that the operator

$$T_m[g](y) = \mathbb{E}_Z \left[g(my + \sqrt{1 - m^2}Z) \right]$$

is diagonal in the *Hermite polynomials* basis [3, Section 2.7.1.] and we have

$$T_m[h_i] = m^i h_i .$$

Thus, by writing f, φ^* in the the Hermite polynomials basis, we obtain

$$\begin{aligned} \mathbb{E}[f(\langle w, X \rangle) \varphi^*(\langle w^*, X \rangle)] &= \mathbb{E}_Y \left[f(Y) \sum_{i=0}^{\infty} a_i^* T_m[h_i](Y) \right] \\ &= \sum_{i=0}^{\infty} \sum_{k=0}^{\infty} a_i^* a_k m^i \mathbb{E}_Y [h_k(Y) h_i(Y)] \\ &= \sum_{k=0}^{\infty} a_k a_k^* m^k, \end{aligned}$$

the proof follows. \square

In this paper, we are interested in two different gradient flows. Their description is the subject of the next section.

B Gradient Flow Dynamics

Gradient flow on $L_\gamma^2 \times \mathcal{S}_{d-1}$. In this section, we derive the equations of motions of the gradient flow on $\mathcal{L}(f, w)$. We say that $(f_t, w_t)_{t \geq 0}$ follow the gradient flow if they are solution of the infinite dimensional system of ODEs

$$\begin{aligned} \frac{d}{dt} f_t &= -\nabla_f^{L_\gamma^2} \mathcal{L}(f_t, w_t), \\ \frac{d}{dt} w_t &= -\nabla_w^{\mathcal{S}_{d-1}} \mathcal{L}(f_t, w_t). \end{aligned}$$

This corresponds to the infinite system of ODEs stated in the Lemma 2 and proven below.

Proof of Lemma 2. We recall the spherical gradient $\nabla_w^{\mathcal{S}_{d-1}} u(w) = \nabla_w u(w) - \langle w, \nabla_w u(w) \rangle w$ for any differentiable function u . Thus, one readily checks that Eq. (6) can be written as

$$\frac{d}{dt} w_t = -(Id - w_t w_t^T) \nabla_w \mathcal{L}(f_t, w_t).$$

Using Eq. (4), we obtain

$$\frac{dm_t}{dt} = \frac{d(w^*)^T w_t}{dt} = (w^*)^T (Id - w_t w_t^T) \sum_{i=1}^{\infty} a_{i,t} a_i^* i m_t^{i-1} w^* = (1 - m_t^2) \sum_{i=1}^{\infty} i a_{i,t} a_i^* m_t^{i-1}.$$

Then, we use the Hilbert property of $(L_\gamma^2, \langle \cdot, \cdot \rangle_{L_\gamma^2})$ and Riesz theorem to the represent the Fréchet differential of $\mathcal{L}(\cdot)$ in terms of a gradient, i.e. for all g sufficiently smooth,

$$\left\langle \nabla_f^{L_\gamma^2} \mathcal{L}(f, w), g \right\rangle_{L_\gamma^2} = \lim_{h \rightarrow 0} \frac{\mathcal{L}(f + hg, w) - \mathcal{L}(f, w)}{h}.$$

A simple calculation leads to

$$\mathcal{L}(f + hg, w) = \mathcal{L}(f, w) + \frac{h^2}{2} \mathbb{E}(g^2(\langle X, w \rangle)) + h \mathbb{E}((f(\langle X, w \rangle) - \varphi^*(\langle X, w^* \rangle))g(\langle X, w \rangle)),$$

and we have

$$\begin{aligned}
\mathbb{E}((f(\langle X, w \rangle) - \varphi^*(\langle X, w^* \rangle))g(\langle X, w \rangle)) &= \mathbb{E}_Y((f(Y) - T_m[\varphi^*](Y))g(Y)) \\
&= \mathbb{E}_Y((f(Y) - \sum_{k=0}^{+\infty} a_k^* m^k h_k(Y))g(Y)) \\
&= \langle f - \sum_{k=0}^{+\infty} a_k^* m^k h_k, g \rangle,
\end{aligned}$$

from which we deduce that

$$\nabla_f^{L_\gamma^2} \mathcal{L}(f, w) = f - \sum_{k=0}^{+\infty} a_k^* m^k h_k = \sum_{k=0}^{+\infty} (a_k - a_k^* m^k) h_k.$$

We recall that *Hermite polynomials* $(h_k)_{k \geq 0}$ form a complete orthonormal basis and we deduce that

$$\frac{da_{k,t}}{dt} = a_k^* m_t^k - a_{k,t}, \quad \forall k \geq 0, t \geq 0$$

with Eq. (5). □

We now turn to the convergence of the flow and the advantage of a coupled dynamics.

C Convergence Behavior of the Joint Gradient Flow

The Planted Model. In this case, the dynamics reduce to a one-dimensional ordinary differential equation for the correlation $m_t := \langle w_t, w^* \rangle$, as previously derived

$$\dot{m}_t = (1 - m_t^2) \sum_{k=1}^{\infty} k (a_k^*)^2 m_t^{k-1}.$$

We show here the Proposition 1 about the planted model. We restate it here for the sake of clarity:

Proposition 1.

- If $m_0 > 0$, the trajectory converges to alignment: $\lim_{t \rightarrow \infty} m_t = 1$.
- If $m_0 < 0$, then, (i) if $s \geq 3$ is odd, we have $\lim_{t \rightarrow \infty} m_t = 0$;
 else, (ii) if s is even, then
 - If $\bar{m} > 1$, the trajectory converges to anti-alignment: $\lim_{t \rightarrow \infty} m_t = -1$.
 - If $\bar{m} < 1$, the trajectory remains trapped in a local minimizer and: $\lim_{t \rightarrow \infty} m_t = -\bar{m}$.

Proof of Proposition 1. If $m_0 > 0$, it is clear that $\dot{m}_t(0) > 0$. By continuity, m_t strictly increases until $(1 - x^2)\Phi(x) = 0$ for $x > 0$, which happens only for $x = 1$, where the system then stabilizes: This follows by combining $\dot{m}_t \geq (1 - m_t^2)s(a^*)^2(m_0)^{s-1}$ with Gronwall's Lemma and $m_t \leq 1$.

If $m_0 < 0$, and $s \geq 3$ is odd, we have $\dot{m}_t(0) > 0$. By continuity, m_t increases until $(1 - x^2)\Phi(x) = 0$ for $x > m_0$, which corresponds to $x = 0$ for m_0 arbitrary small. By Picard–Lindelöf theorem, we have uniqueness of the solutions and thus $m_t < 0$. We deduce that $\dot{m}_t \geq c(m_t)^{s-1}$, which lead to the convergence to 0 by Gronwall's Lemma.

If s is even, then, we have $\dot{m}_t(0) < 0$. By continuity, m_t decreases until $(1 - x^2)\Phi(x) = 0$ for

$x \leq m_0$, which corresponds to $x = -\bar{m}$ if $\bar{m} < 1$ or $x = -1$ if $\bar{m} > 1$. In the case where $\bar{m} < 1$, by Picard–Lindelöf theorem, $m_t > -\bar{m}$ and we conclude by noting that m_t cannot converge to a larger $\alpha > -\bar{m}$. If it did, as m_t is decreasing, α should be a zero of $\Phi(x)$. The case $\bar{m} > 1$ follows by a similar argument. \square

Proposition 1 highlights the limitations of the planted model. The joint dynamics does not suffer from such issues.

C.1 Main theorem: convergence in the Joint Learning Setting

We now move on to solving the system of differential equations (8)-(9). Note that if $a_k^* = 0$, $a_{k,t}$ tends exponentially fast to 0 by (8) and the dynamics of m_t is independent of such $a_{k,t}$. Therefore, from now on, we are interested only in the $a_{k,t}$ such that $a_k^* \neq 0$. *In passing*², we mention that $f_t \in L_\gamma^2$ for all $t \geq 0$. Indeed, the following states that the $a_{k,t}$ remain within $[-\max(|a_k^*|, |a_{k,0}|), \max(|a_k^*|, |a_{k,0}|)]$. Indeed,

Fact 1. *We have $|a_{k,t}| \leq \max(|a_k^*|, |a_{k,0}|)$. If $|a_{k,t}| \leq |a_k^*|$ for some t , then for $t' \geq t$, $|a_{k,t'}| \leq |a_k^*|$. Finally, If it does not exist t such that $|a_{k,t}| \leq |a_k^*|$, then $a_{k,t}$ tends exponentially fast to a_k^* (monotonically). Hence, for all $t \geq 0$, $f_t \in L_\gamma^2$ and the flow is well defined at all times.*

Proof. Using (8), it follows that

$$\frac{da_{k,t}}{dt} \geq 0 \iff a_k^* m_t^k \geq a_{k,t} \implies \begin{array}{l} a_k^* \geq a_{k,t} \text{ if } a_k^* > 0. \\ -a_k^* \geq a_{k,t} \text{ if } a_k^* < 0, \end{array} \implies |a_{k,t}| \geq a_{k,t}$$

by using the fact that $|m_t| \leq 1$ and in the same way, $\frac{da_{k,t}}{dt} \leq 0$ implies that $a_{k,t} \geq -|a_k^*|$. We conclude the proof of the first two points. We now address the third point. For $m_0 > 0$ and $a_{k,0} > a_k^* > 0$, we have

$$\frac{da_{k,t}}{dt} \leq a_k^* - a_{k,t},$$

and by Grönwall's lemma, we obtain that

$$a_{k,t} \leq a_k^* + (-a_k^* + a_{k,0})e^{-t}.$$

By hypothesis $a_{k,t} \geq a_k^*$, which concludes the proof for this case. The other cases work in the same way. \square

We are now in a position to establish the main theorem.

Proof of Theorem 1. We divide the proof of the theorem into two subsections, the case $s \geq 2$ and the case $s = 1$. The remainder of the appendix is devoted to the proof of this Theorem: The argument proceeds through several key lemmas, which we state and prove below before completing the proof of the theorem.

C.1.1 Proof of Theorem 1 for $s \geq 2$

In all the following, we define for all $\kappa \in (0, 1)$, the time at which m attains level set $\kappa > 0$.

$$\tau_\kappa = \inf\{t \geq 0 \mid |m_t| \geq \kappa\}.$$

Denote $u_{k,t} = a_{k,t} - a_k^* m_t^k$ and write $\bar{m}_{[t,t_0]} = \sup_{t_0 \leq s \leq t} |m_s|$. The goal of the next lemmas is to show that, after a time of order $\log(1/m_0)$, m_t has barely moved, while an arbitrary number of $a_{k,t}$ are nearly equal to $a_k^* m_t^k$.

²as we say in the London Society Club of French Gentlemen.

Lemma 3. *There exists $C > 0$, such that for all $k \geq s$, and all $t \geq t_0$, we have*

$$|a_{k,t} - a_k^* m_t^k| \leq C \bar{m}_{[t,t_0]}^{k+s-2} + |a_{k,t_0} - a_k^* m_{t_0}^k| e^{-(t-t_0)} \quad (21)$$

Proof. We have for all $k \geq s, t \geq 0$,

$$\begin{aligned} \dot{u}_{k,t} &= \dot{a}_{k,t} - k a_k^* m_t^{k-1} \dot{m}_t \\ &= -u_{k,t} - k a_k^* m_t^{k-1} (1 - m_t^2) \sum_{k \geq s} k a_{k,t} a_k^* m_t^{k-1}. \end{aligned}$$

That is to say that

$$\begin{aligned} |\dot{u}_{k,t} + u_{k,t}| &= \left| k a_k^* m_t^{k-1} (1 - m_t^2) \sum_{j \geq s} j a_{j,t} a_j^* m_t^{j-1} \right| \\ &\leq k |a_k^*| |m_t|^{k-1} (1 - m_t^2) \sum_{j \geq s} j |a_{j,t} a_j^*| |m_t|^{j-1} \\ &\leq k |a_k^*| |m_t|^{k-1} |m_t|^{s-1} \sum_{j \geq s} j |a_{j,t} a_j^*| |m_t|^{j-s}, \end{aligned}$$

and using $|a_{j,t}| \leq |a_{j,0}| + |a_j^*|$, we get

$$\begin{aligned} |\dot{u}_{k,t} + u_{k,t}| &\leq k |a_k^*| |m_t|^{k+s-2} \sum_{j \geq s} j (|a_j^*|^2 + |a_{j,0} a_j^*|) \\ &\leq k |a_k^*| |m_t|^{k+s-2} \sum_{j \geq s} j (2|a_j^*|^2 + |a_{j,0}|^2) \\ &\leq C |m_t|^{k+s-2}, \end{aligned}$$

where C is a uniform in k upperbound on $k |a_k^*| \sum_{j \geq s} j (|a_j^*|^2 + |a_{j,0} a_j^*|)$. Applying the Gronwall inequality between t and t_0 , we have that

$$|u_{k,t} - u_{k,t_0} e^{-(t-t_0)}| \leq C e^{-t} \int_{t_0}^t |m_u|^{k+s-2} e^u du \leq C \bar{m}_{[t,t_0]}^{k+s-2},$$

which ends the proof of the lemma. \square

Let $k^* \geq s$ an integer that we consider large enough, with no dependency on the dimension though. Define $t_{k^*} = C k^* \ln(1/m_0)$. The first step is to establish that m_t stays near its initial value m_0 for a duration of order $m_0^{1-s} \gg t_{k^*}$ and that $\dot{m}_{t_{k^*}}$ has the sign of the initial value.

Lemma 4. *At time t_{k^*} , for all $k \leq k^*$, we have $a_{k,t_{k^*}} a_k^* m_{t_{k^*}}^k > 0$. Moreover,*

- if $m_0 > 0$, then $C m_0 > m_t > c m_0$ for $t \leq \frac{c}{m_0^{s-1}}$ and $\dot{m}_{t_{k^*}} > 0$,
- if $m_0 < 0$, then $-C m_0 < m_t < -c m_0$ for $t \leq \frac{c}{m_0^{s-1}}$ and $\dot{m}_{t_{k^*}} < 0$.

Then, after time t_{k^*} , the $a_{k,t}$ for $k \leq k^*$ have concentrated near their equilibrium $a_k^* m_t^k$ and, therefore it is possible to reinforce the lemma 3 with the following version.

Lemma 5. *There exist constants $C, c > 0$, such that for all $s \leq k \leq k^*$, and all $t \geq t_{k^*}^*$, we have*

$$|a_{k,t} - a_k^* m_t^k| \leq C \bar{m}_{[t,t_{k^*}]}^{k+2s-2}. \quad (22)$$

Proof of Lemma 4. The first step is to establish that m_t stays near its initial value m_0 for a duration of order $m_0^{1-s} \gg t_{k^*}$. We first consider $m_0, a_s^* > 0$ and define $\tau = \inf\{t \geq 0, m_t \geq Cm_0 \text{ or } m_t \leq cm_0\}$. For $t \leq \tau$, by using (8), we obtain

$$ca_s^* m_0^s - a_{2,t} \leq \frac{da_{s,t}}{dt} \leq Ca_s^* m_0^s - a_{2,t},$$

from which we deduce that

$$ca_s^* m_0^s + (-a_s^* cm_0^s + a_{s,0})e^{-t} \leq a_{s,t} \leq a_s^* Cm_0^s + (-a_s^* Cm_0^s + a_{s,0})e^{-t}.$$

The previous inequality can be readily adapted to various cases: In the case where $a_s^* m_0^s < 0$, we interchange C and c . In our case, by using (9) for $t \leq \tau$, we have

$$ce^{-t} m_0^{s-1} + cm_0^s - C \sum_{k=s+1} m_t^{k-1} \leq \frac{dm_t}{dt} \leq Ce^{-t} m_0^{s-1} + Cm_0^s + C \sum_{k=s+1} m_t^{k-1}.$$

All in all, we get

$$cm_0^{s-1} - Cm_0^s t + m_0 \leq m_t \leq Cm_0^{s-1} + Cm_0^s t + m_0,$$

from which we conclude that

$$\frac{c}{m_0^{s-1}} \leq \tau \leq \frac{C}{m_0^{s-1}}.$$

Meanwhile, we now prove that $a_{k,t}$ is the sign of $a_k^* m_0^k$ at t_{k^*} . Let $a_k^* > 0$, by using (8), we get that for $t \leq \tau$

$$\frac{da_{k,t}}{dt} \geq a_k^* (cm_0)^k - a_{k,t}, \quad (23)$$

and by Gronwall's lemma, we have

$$a_{k,t} \geq a_k^* (cm_0)^k + (-a_k^* (cm_0)^k + a_{k,0})e^{-t},$$

which proves that $a_{k,t}$ is strictly positive exponentially fast. More precisely, $a_{k,t} \geq a_k^* (cm_0)^k / 2$ in a time smaller than

$$\log \left(\frac{2(a_k^* (cm_0)^k - a_{k,0})}{a_k^* (cm_0)^k} \right),$$

which is order $k \log(1/m_0) \ll cm_0^{1-s}$. The case $a_k^* < 0$ works the same way by noting that the inequality (23) is true in the opposite direction. The case where m_0 is negative is very similar and is left to the reader. Thus, at time t_{k^*} , $m_{t_{k^*}} > 0$ and $a_{k,t_{k^*}} a_k^* m_{t_{k^*}}^k > 0$. In addition, we have

$$\frac{dm_t}{dt} = (1 - m_t^2) \sum_{i=s}^{k^*} ia_{i,t} a_i^* m_t^{i-1} + (1 - m_t^2) \sum_{i=k^*+1}^{+\infty} ia_{i,t} a_i^* m_t^{i-1} > 0 \text{ for } t = t_{k^*},$$

since all the terms in the first sum are positive and the first summand is at least of order m_0^{2s-1} while the second sum is at most of order $m_0^{k^*}$. \square

Proof of Lemma 5. From equality Eq.(21), taken between 0 and $t \geq t_{k^*}$, we have

$$\begin{aligned} |a_{k,t}| &\leq |a_k^* m_t^k| + C \bar{m}_{[t,0]}^{k+s-2} + C m_0^{Ck^*} \\ &\leq |a_k^* \bar{m}_{[t,0]}^k| + C \bar{m}_{[t,0]}^{k+s-2} \\ &\leq C |\bar{m}_{[t,0]}^k| \\ &\leq C |\bar{m}_{[t,t_{k^*}]}^k|. \end{aligned}$$

The last inequality by lemma (4). Then, we estimate

$$\begin{aligned} \sum_{j \geq s} j |a_{j,t} a_j^*| |m_t|^{j-1} &\leq C |m_t|^{s-1} \bar{m}_{[t,t_{k^*}]}^s \sum_{j \geq s} j \bar{m}_{[t,t_{k^*}]}^{j-s} |a_j^*| |m_t|^{j-s} \\ &\leq C \bar{m}_{[t,t_{k^*}]}^{2s-1} \sum_{j \geq s} j |a_j^*| |\bar{m}_{[t,t_{k^*}]}|^{2(j-s)} \\ &\leq C \bar{m}_{[t,t_{k^*}]}^{2s-1}. \end{aligned}$$

Notice that in this estimation, we have hence gained a factor s compared to before. This gives

$$\begin{aligned} |\dot{u}_{k,t} + u_{k,t}| &= \left| k a_k^* m_t^{k-1} (1 - m_t^2) \sum_{j \geq s} j a_{j,t} a_j^* m_t^{j-1} \right| \\ &\leq k |a_k^*| |m_t|^{k-1} \sum_{j \geq s} j |a_{j,t} a_j^*| |m_t|^{j-1} \\ &\leq C |m_t|^{k-1} \bar{m}_{[t,t_{k^*}]}^{2s-1} \\ &\leq C \bar{m}_{[t,t_{k^*}]}^{k+2s-2}, \end{aligned}$$

that we integrate between t_{k^*} and t . Then, the end of the proof follows the same way as before. \square

Hence we can define

$$\begin{aligned} \tilde{\tau}_{k^*} &= \inf\{t \geq t_{k^*} \mid \forall k \leq k^*, a_{k,t_{k^*}} a_k^* m_{t_{k^*}}^k \leq 0 \text{ or } \dot{m}_t \text{ changes sign}\} \\ &= \inf\{t \geq t_{k^*} \mid \forall k \leq k^*, a_{k,t} \text{ changes sign or } a_k^* m_t^k \text{ changes sign or } \dot{m}_t \text{ changes sign}\}. \end{aligned} \quad (24)$$

We will prove eventually that $\tilde{\tau}_{k^*} = +\infty$. Before this, we prove quantitatively that there exists a constant $c > 0$, so that after a time of order $m_0^{2(1-s)}$, m reaches level c .

Lemma 6. *There exists $b, B > 0$, such that $b/m_0^{2(s-1)} \leq \tau_c \leq B/m_0^{2(s-1)}$, moreover $\tilde{\tau}_{k^*} \geq \tau_c$.*

We postpone the proof of Lemma 6 for after. By the inequality Eq.(21), as m has reached a constant level $c > 0$, this means that all $k \leq k^*$, this is also the case for the $a_{k,(\cdot)}$. Let us define the constants, for all $k \leq k^*$,

$$c_k = \frac{1}{2} \min\{|a_{k,\tau_c}|, |a_k^* m_{\tau_c}^k|\}, \text{ and the times } \bar{\tau}_k = \inf\{t \geq \tau_c \mid |a_{k,t}| \leq c_k\}.$$

Lemma 7. *For all $k \leq k^*$, we have $\bar{\tau}_k = \tilde{\tau}_{k^*} = +\infty$.*

Proof. To fix the ideas, we fix a $k \leq k^*$ and assume $a_k^* > 0$ as well as the case $m_0 > 0$. For all $t \in [\tau_c, \min_k \bar{\tau}_k]$, $\dot{m}_t > 0$ if $\sum_{k \geq s} k a_{k,t} a_k^* m_t^{k-1} > 0$, but we instantly see, that this is the case splitting the sum before k^* which as a positive and constant contribution and after that can be as small as we want by choosing a large k^* . Hence, m increases strictly in $[\tau_c, \min_k \bar{\tau}_k]$. Furthermore, $\dot{a}_{k,t} = a_k^* m_t^k - a_{k,t}$, so that either $a_{k,t} \geq a_k^* m_t^k > a_k^* m_{\tau_c}^k > c_k$ or in the other case $\dot{a}_{k,t} > 0$, and hence $a_{k,t} \geq \min\{a_k^* m_{\tau_c}^k, a_{k,\tau_c}\} > c_k$. Either case, if $\min_k \bar{\tau}_k < \infty$, this leads to a contradiction. Finally, as we have seen that m increases strictly in $[\tau_c, \min_k \bar{\tau}_k]$ and that all $a_{k,(\cdot)}$ are lower bounded by a constant, $\tilde{\tau}_{k^*} \geq \min_k \bar{\tau}_k = +\infty$. \square

We move to the convergence of the coefficients $(a_{k,t})$ and m_t for $s \geq 2$, thereby addressing the first part of Theorem 1.

Theorem 2. *There exists constants $c, C > 0$ so that after time $t \geq \tau_c \geq \frac{C}{m_0^{2(s-1)}}$,*

$$\begin{aligned} \bullet \text{ if } m_0 > 0, & \quad |1 - m_t| \leq Ce^{-c(t-\tau_c)}, \\ & \quad |a_{k,t} - a_k^*| \leq Cb_k e^{-c(t-\tau_c)}, \text{ for all } k \in \mathbb{N}, \\ \bullet \text{ if } m_0 < 0, & \quad |1 + m_t| \leq Ce^{-c(t-\tau_c)}, \\ & \quad |a_{k,t} - (-1)^k a_k^*| \leq Cb_k e^{-c(t-\tau_c)}, \text{ for all } k \in \mathbb{N}, \end{aligned}$$

where, $b \geq 0$ is a normalized sequence of $\ell_2(\mathbb{N})$, i.e. $\|b\|_{\ell_2(\mathbb{N})} = 1$.

Proof. Let us first show the contraction of m . Assume that we are in the case where $m_0 > 0$, define $v_t = 1 - m_t \geq 0$, for all $t \geq \tau_c$, we have

$$\dot{v}_t = -(1 - m_t^2) \sum_{k \geq s} k a_{k,t} a_k^* m_t^{k-1} \leq -v_t (2c - \sum_{k \geq k^*} k |a_{k,t} a_k^* m_t^{k-1}|),$$

but once again this latter sum can be made arbitrarily small choosing a large k^* , so that

$$\dot{v}_t \leq -cv_t,$$

and the first inequality comes from Gronwall lemma. For the contraction of the a , we pose $z_{k,t} = |a_{k,t} - a_k^*|^2$, and for all $t \geq \tau_c$,

$$\begin{aligned} \frac{d}{dt} z_{k,t} &= 2(a_{k,t} - a_k^*)(a_k^* m_t^k - a_{k,t}) \\ &= -2z_{k,t} + 2a_k^*(a_{k,t} - a_k^*)(m_t^k - 1) \\ &= -2z_{k,t} + 2a_k^*(a_{k,t} - a_k^*)(m_t - 1) \sum_{i=1}^k m_t^i, \end{aligned}$$

so that we have

$$|\dot{z}_{k,t} + 2z_{k,t}| \leq Ck |a_k^*| \sqrt{z_{k,t}} e^{-c(t-\tau_c)}$$

Defining $\bar{z}_{k,t} = \sqrt{z_{k,t+\tau_c}}$, we have that is satisfies, for all $t \geq 0$,

$$|\dot{\bar{z}}_{k,t} + \bar{z}_{k,t}| \leq Cb_k e^{-ct},$$

where $\|b\|_{\ell_2(\mathbb{N})} = 1$ which integrates in close forme and gives a solution that is upper bounded by $\bar{z}_{k,t} \leq Cb_k e^{-ct}$, and this finishes the proof of the theorem in the case $m_0 > 0$.

For the sake of clarity we draw the lines of the case $m_0 < 0$ but there are essentially the same. Define $v_t = 1 + m_t \geq 0$, for all $t \geq \tau_c$, we have

$$\dot{v}_t = v_t(1 - m_t) \sum_{k \geq s} k a_{k,t} a_k^* m_t^{k-1} \leq v_t (-2c + \sum_{k \geq k^*} k |a_{k,t} a_k^* m_t^{k-1}|),$$

but once again this latter sum can be made arbitrarily small choosing a large k^* , so that

$$\dot{v}_t \leq -cv_t,$$

and the first inequality comes from Gronwall lemma. For the contraction of the a , if k is even, we pose $z_{k,t} = |a_{k,t} - a_k^*|^2$, and for all $t \geq \tau_c$,

$$\frac{d}{dt} z_{k,t} = -2z_{k,t} + 2a_k^*(a_{k,t} - a_k^*)(m_t + 1)(m_t - 1) \sum_{i=1}^{k/2} m^{2i},$$

so that we have

$$|\dot{z}_{k,t} + 2z_{k,t}| \leq Ck|a_k^*|\sqrt{z_{k,t}}e^{-c(t-\tau_c)}$$

and the proof ends as before. Now, if k is odd, we pose $z_{k,t} = |a_{k,t} + a_k^*|^2$, and for all $t \geq \tau_c$,

$$\begin{aligned} \frac{d}{dt} z_{k,t} &= -2z_{k,t} + 2a_k^*(a_{k,t} + a_k^*)(m_t^k + 1) \\ &= -2z_{k,t} + 2a_k^*(a_{k,t} + a_k^*)(m_t + 1) \sum_{i=1}^k (-1)^i m^i \end{aligned}$$

so that we have

$$|\dot{z}_{k,t} + 2z_{k,t}| \leq Ck|a_k^*|\sqrt{z_{k,t}}e^{-c(t-\tau_c)}$$

and the proof ends, once again, as before. This final case concludes the proof of the theorem. \square

We finish this section by proving Lemma 6.

Proof of Lemma 6. Let us assume first that $m_0 > 0$, the case where $m_0 < 0$, is symmetric by multiplying by -1 (and thus reverting) all inequalities below. Then, after time t_{k^*} , by Lemma 4, we have $m_{t_{k^*}} > 0$ as well as $\dot{m}_{t_{k^*}} > 0$. By continuity of all processes involved, we know that $\tilde{\tau}_{k^*} > t_{k^*}$. Then, for all $t \in [t_{k^*}, \tilde{\tau}_{k^*}]$, as m increases, we have $m_t = \bar{m}_{[t, t_{k^*}]}$ and

$$\begin{aligned} \dot{m}_t &= (1 - m_t^2) \sum_{k \geq s} k a_{k,t} a_k^* m_t^{k-1} \\ &\geq \frac{3}{4} \sum_{k=s}^{k^*} k a_{k,t} a_k^* m_t^{k-1} + \frac{3}{4} \sum_{k \geq k^*+1} k a_{k,t} a_k^* m_t^{k-1} \\ &\geq \frac{3}{4} s a_{s,t} a_s^* m_t^{s-1} - \frac{3}{4} \sum_{k \geq k^*+1} k |a_{k,t} a_k^* m_t^{k-1}|. \end{aligned}$$

From there, by Lemma 5 applied between t_{k^*} and t , we have

$$a_s^* m_t^s - C \bar{m}_{[t, t_{k^*}]}^{3s-2} \leq a_{s,t} \leq a_s^* m_t^s + C \bar{m}_{[t, t_{k^*}]}^{3s-2},$$

and hence we have

$$a_{s,t} a_s^* m_t^{s-1} \geq |a_s^*|^2 m_t^{2s-1} - C |a_s^*| m_t^{3s-1},$$

so that

$$\begin{aligned} \dot{m}_t &\geq \frac{3s|a_s^*|^2}{4} m_t^{2s-1} - \frac{3sC|a_s^*|}{4} m_t^{3s-1} - \frac{3}{4} \sum_{k \geq k^*+1} k |a_{k,t} a_k^* m_t^{k-1}| \\ &\geq b m_t^{2s-1} - b C m_t^{3s-1} - C m_t^{k^*} \sum_{k \geq k^*+1} k |a_{k,0} a_k^*| \\ &\geq b m_t^{2s-1} - b C m_t^{3s-1} \\ &\geq b m_t^{2s-1} (1 - C m_t^{s-1}). \end{aligned}$$

Hence, for $s \geq 2$, there exists a constant $c > 0$, such that for all $t \in [t_{k^*}, \tilde{\tau}_{k^*} \wedge \tau_c]$,

$$\dot{m}_t \geq cm_t^{2s-1}.$$

Let us assume that $\tilde{\tau}_{k^*} < \tau_c$, then either

- $m_{\tilde{\tau}_{k^*}} = 0$, which is impossible because in virtue of the inequality above m is increasing between t_{k^*} and $\tilde{\tau}_{k^*}$.
- $\dot{m}_{\tilde{\tau}_{k^*}} = 0$, and hence $m_{\tilde{\tau}_{k^*}} = 0$ which is impossible because of the bullet point above.
- $a_{k, \tilde{\tau}_{k^*}} = 0$, which is impossible because for all $t \in [t_{k^*}, \tilde{\tau}_{k^*} \wedge \tau_c]$, in the case $a_k^* > 0$,

$$\dot{a}_{k, \tilde{\tau}_{k^*}} = a_k^* m_{\tilde{\tau}_{k^*}}^k > a_k^* m_0^k > 0,$$

which is a contraction since $a_{k,t}$ cannot cross from positive to negative with a positive speed. The case where $a_k^* < 0$ is exactly similar.

Hence, finally, $\tilde{\tau}_{k^*} \geq \tau_c$, and for all $t \in [t_{k^*}, \tau_c]$, $\dot{m}_t \geq cm_t^{2s-1}$. This means that $\tau_c \leq t_{k^*} + C/m_0^{2(s-1)}$.

For the lower bound, this rests on the same argument as for $t \geq t_{k^*}$,

$$\begin{aligned} \dot{m}_t &= (1 - m_t^2) \sum_{k \geq s} ka_{k,t} a_k^* m_t^{k-1} \\ &\leq sa_{s,t} a_s^* m_t^{s-1} + m_t^s \sum_{k \geq s+1} ka_{k,t} a_k^* m_t^{k-s} \\ &\leq bm_t^{2s-1} + bCm_t^{2s} \\ &\leq Cm_t^{2s-1}, \end{aligned}$$

up to a constant level $c > 0$, if c is a small enough constant. This ends the proof of the lemma. \square

C.2 Proof of Theorem 1 for $s = 1$

The case $s = 1$ is somewhat different. In the case $s \geq 2$, m_t initially remains very close to m_0 , allowing the coefficients $a_{k,t}$ to adopt the sign of their target values (the sign of $a_k^* m_t^k$). In contrast, in the case $s = 1$, m_t initially moves linearly toward the sign of $a_{1,0} a_1^*$ in an initial phase and only after that do the coefficients $a_{k,t}$ adopt the sign of their target values: the sign of $a_k^* m_t^k$.

Lemma 8. *There exists a time $T \geq C$ independent of m_0 , such that both m_T and $a_{1,T}$ are bounded away from zero by a constant independent of m_0 . Moreover, m_T has the sign of $a_{1,0} a_1^*$, while $a_{1,T}$ has the sign of $a_{1,0}$.*

Proof. We prove that $a_{1,t}$ does not have time to reach 0, as m_t is already far from 0 in the direction of $a_1^* a_{1,0}$. Let

$$T_1 = \inf\{t \geq 0, |a_{1,t} - a_{1,0}| \geq \frac{|a_{1,0}|}{2}\}.$$

By using (8), for all $t \leq T_1$, we obtain that

$$|a_{1,t} - a_{1,0}| \leq \int_0^t \left| \frac{da_{1,u}}{du} \right| du \leq \int_0^t (|a_1^*| + |a_{1,u}|) du \leq t(|a_1^*| + \frac{3}{2}|a_{1,0}|).$$

We deduce $T_1 \geq |a_{1,0}| / (2(|a_1^*| + \frac{3}{2}|a_{1,0}|))$, which is of order 1. Meanwhile, for $t \leq T_1 \wedge \tau_{1/2}$, we have that

$$c_1 a_1^* a_{1,0} - C|m_t| \leq \frac{dm_t}{dt} \leq c_2 a_1^* a_{1,0} + C|m_t|$$

where $c_1 = 1/2, c_2 = 3/2$ if $a_1^* a_{1,0} > 0$ and the contrary else. Let

$$T_2 = \inf\{t \geq 0, |m_t| > \min(1/2, |a_1^* a_{1,0}|/4C)\}.$$

We thus deduce that for $t \leq T_1 \wedge T_2 =: T$,

$$c_3 a_1^* a_{1,0} t + m_0 \leq m_t \leq c_4 a_1^* a_{1,0} t + m_0,$$

where $c_3, c_4 > 0$. We deduce that after a time of order m_0 , m_t is a sign of $a_{1,0} a_1^*$. At time T , m_t and $a_{1,t}$ are of order 1 and both have the sign of $a_{1,0}$. \square

We now prove that, after time T , both m_t and $a_{1,t}$ remain uniformly bounded away from zero.

Lemma 9. *There exists constants $c, C > 0$ so that after time $t \geq C$, $|m_t|, |a_{1,t}| \geq c$. Moreover,*

- if $a_1^* a_{1,0} > 0$, then $m_t > c$,
- if $a_1^* a_{1,0} < 0$, then $m_t < -c$.

Proof. Without loss of generality, we consider $a_{1,0} < 0$, and $a_1^*, m_0 > 0$. From $t \geq T$, we recall that $a_{1,t}, m_t < 0$ and of order 1. However, from here, m_t is free to increase or decrease for a certain time. We now prove that m_t is however bounded away from 0 by a constant $-\delta$ independent of m_0 . By defining

$$\tilde{T}_\delta = \inf\{t \geq T, a_1^* m_t \geq -\delta\},$$

for $-\delta > m_T$ small enough: First, we require $\frac{a_{1,0}}{2} < -\delta$ to have $a_{1,T} < -\delta$. Then, we claim that $a_1^* m_t$ must reach $-\delta$ before $a_{1,t}$ does. Indeed, by recalling that

$$\frac{da_{1,t}}{dt} = a_1^* m_t - a_{1,t}, t \geq 0,$$

we deduce that in order to hit $-\delta$, a_t has to be in an increasing phase, that is $a_1^* m_t \geq a_{1,t}$ from which we deduce that $a_1^* m_t$ must reach $-\delta$ before $a_{1,t}$. We first prove that $\tilde{T}_\delta \geq -c \log(\delta)$. Indeed for $\tilde{T}_{\sqrt{\delta}} \leq t \leq \tilde{T}_\delta$ (we require also $\frac{a_{1,0}}{2} < -\sqrt{\delta}$), we have

$$\frac{da_{1,t}}{dt} \leq -\delta - a_{1,t},$$

which implies that for $t \geq \tilde{T}_{\sqrt{\delta}}$

$$a_{1,t} \leq -\delta + (a_{1,\tilde{T}_{\sqrt{\delta}}} + \delta) e^{-(t-\tilde{T}_{\sqrt{\delta}})} \leq -\delta + (-\sqrt{\delta} + \delta) e^{-(t-\tilde{T}_{\sqrt{\delta}})},$$

from which we deduce that $\tilde{T}_\delta \geq -c \log(\delta)$. We recall that for $t \leq \tau_{1/2}$, it exists C such that

$$\frac{dm_t}{dt} \leq a_1^* a_{1,t} + 2a_2^* a_{2,t} m_t + C m_t^2,$$

and thus we obtain

$$\left. \frac{dm_t}{dt} \right|_{t=\tilde{T}_\delta} \leq a_1^* a_{1,\tilde{T}_\delta} - 2a_2^* a_{2,\tilde{T}_\delta} \delta / a_1^* + C(\delta/a_1^*)^2 \leq -a_1^* \delta - 2a_2^* a_{2,\tilde{T}_\delta} \delta / a_1^* + C(\delta/a_1^*)^2.$$

To conclude, we consider an adversarial case where $a_2^* > 0$ and $a_{2,t} < 0$, and we deduce that $\left. \frac{dm_t}{dt} \right|_{t=\tilde{T}_\delta}$ is negative because $a_{2,t} \geq -(a_1^*)^2 / (4a_2^*)$ in a time independent of δ (see $\frac{da_{2,t}}{dt} \leq -a_{2,t}$). \square

We now prove that an arbitrary number of coefficients $a_{k,t}$ adopt the sign of their target values (the sign of $a_k^* m_t^k$).

Lemma 10. For $k^* > 0$, it exists $t_{k^*} \geq C$, for all $k \leq k^*$, we have $a_{k,t_{k^*}} a_k^* m_{t_{k^*}}^k > 0$.

Proof. The proof is very similar to the proof of Lemma 4. We now return to our prototypical example : Let $a_{1,0} < 0$, and $a_1^*, m_0 > 0$. Consider $a_{2k}^* > 0$, using Lemma 9, for $t \geq T$, we have

$$\frac{da_{2k,t}}{dt} \geq a_{2k}^* \delta^{2k} - a_{2k,t},$$

which implies, by Gronwall's lemma, that

$$a_{2k,t} \geq a_{2k}^* \delta^{2k} + (-a_{2k}^* \delta^{2k} + a_{2k,0}) e^{-t},$$

which proves that $a_{2k,t}$ is strictly positive exponentially fast. The other cases work similarly. Thus, at time t_{k^*} , $m_{t_{k^*}} < 0$ by Lemma 9 and $a_{k,t_{k^*}} a_k^* m_{t_{k^*}}^k > 0$ for $k \leq k^*$. \square

We move to the convergence of $m_t, (a_{k,t})$.

Theorem 3. There exists constants $c, C > 0$ so that after time $t \geq 0$,

$$\begin{aligned} \bullet \text{ if } a_1^* a_{1,0} > 0, & \quad |1 - m_t| \leq C e^{-ct}, \\ & \quad |a_{k,t} - a_k^*| \leq C b_k e^{-ct}, \text{ for all } k \in \mathbb{N}, \\ \bullet \text{ if } a_1^* a_{1,0} < 0, & \quad |1 + m_t| \leq C e^{-ct}, \\ & \quad |a_{k,t} - (-1)^k a_k^*| \leq C b_k e^{-ct}, \text{ for all } k \in \mathbb{N}, \end{aligned}$$

where, $b \geq 0$ is a normalized sequence of $\ell_2(\mathbb{N})$, i.e. $\|b\|_{\ell_2(\mathbb{N})} = 1$.

Proof. Assume that we are in the case where $a_{1,0} < 0$, and $a_1^*, m_0 > 0$. We recall that

$$\frac{dm_t}{dt} = (1 - m_t^2) \sum_{i=s}^{k^*} i a_{i,t} a_i^* m_t^{i-1} + (1 - m_t^2) \sum_{i=k^*+1}^{+\infty} i a_{i,t} a_i^* m_t^{i-1}.$$

At time $t = t_k^*$, by Lemma 9 and Lemma 10, the first sum on the right-hand side of the latter equation is negative. Using (8), we immediately see that $a_{k,t}$, $k \leq k^*$ cannot change sign for $t \geq t_k^*$: The derivative $\frac{da_{k,t}}{dt}$ has the sign of $a_k^* m_t^k$ for $a_{k,t} = 0$. Define $v_t = 1 + m_t \geq 0$, for all $t \geq t_{k^*}$, we have

$$\dot{v}_t = (1 - m_t^2) \sum_{k \geq s} k a_{k,t} a_k^* m_t^{k-1} \leq v_t (-c + \sum_{k \geq k^*} k |a_{k,t} a_k^* m_t^{k-1}|),$$

because $a_{1,t} < -c$. But once again this latter sum can be made arbitrarily small choosing a large k^* , so that

$$\dot{v}_t \leq -c v_t,$$

and the first inequality comes from Gronwall lemma. For the contraction of a 's, we do exactly as in the proof of Theorem 2. \square

The proof of Theorem 1 follows. \square